2010

Fundamental Optimal Performance Design Guidelines for Off-Set Type Reciprocating Compressors to Maximize Mechanical Efficiency

Takuma Tsuji
Osaka Electro-Communication University

Noriaki Ishii
Osaka Electro-Communication University

Keiko Anami
Dept. Mechanical Engineering

Kiyoshi Sawai
Appliances Development Center

Akira Hiwata
Appliances Development Center

See next page for additional authors

Authors
Takuma Tsuji, Noriaki Ishii, Keiko Anami, Kiyoshi Sawai, Akira Hiwata, Takashi Morimoto, Kiyoshi Sano, and Charles Knisely

Fundamental Optimal Performance Design Guidelines for Off-Set Type Reciprocating Compressors to Maximize Mechanical Efficiency

Takuma TSUJI[1]*, Noriaki ISHII[1], Keiko ANAMI[2], Kiyoshi SAWAI[3], Akira HIWATA[3]
Takashi MORIMOTO[3], Kiyoshi SANO[3] and Charles W. KNISELY[4]

[1]Osaka Electro-Communication Univ., Dept. of Mechanical engineering,
Osaka, Japan.
Tel/fax: +81-72-820-4561, E-mail: ishii@isc.osakac.ac.jp

[2]Ashikaga Institute of Technology, Dept. of Mechanical engineering,
Tochigi, Japan.
Tel/fax: +81-284-62-0605, E-mail: anami@ashitech.ac.jp

[3]Appliances Development Center, Corporate Engineering Division, Home Appliances Company,
Panasonic Corporation.
Shiga, Japan
Tel: +81-77-562-5658, fax: +81-77-563-1967

[4]Bucknell Univ., Dept. of Mechanical Engineering
Lewisburg, Pennsylvania, USA
Tel: 570-577-1817, fax: 570-577-7281, E-mail: knisely@bucknell.edu

ABSTRACT

Optimal design guidelines for reciprocating compressors, one of the earliest classical compression devices, are less well developed. This paper first provides a review of the optimal design guidelines for rotary and scroll compressors. Then subsequently a parametric computer simulation study of the mechanical efficiency of compact off-set type reciprocating refrigerant compressors is presented. From the computer simulations, fundamental optimal performance design guidelines for maximum mechanical efficiency are identified. The frictional power loss at each pair of compressor elements depends mainly upon the corresponding constraint force. The constraint forces depend not only upon the compression pressure and the inertia forces but also upon the combination of piston diameter and stroke for a given suction volume. The suction volume for a given reciprocating compressor is determined by these major parameters. Consequently, there are many combinations of major parameters that result in a reciprocating compressor with the same suction volume. Therefore, the constraint force and the frictional power loss at each element pair change, depending upon the selected combination of major parameters, thereby resulting in a different mechanical efficiency. Thus, selection of the optimum combination of major parameters is necessary to ensure maximum mechanical efficiency of the reciprocating compressor. The mechanical efficiency of a small capacity reciprocating compressor with a variety of piston off-set was calculated, where the combination of piston diameter and stroke was varied for a fixed suction volume. The calculated results indicate that there is an optimum combination of these major parameters. In addition, the physical basis for the optimum combination of major parameters was examined by showing the characteristics of the frictional power loss at each element pair.

1. INTRODUCTION

While optimal design guidelines have been developed and documented for scroll and rolling-piston rotary refrigerant compressors (see references [1 to 14] for scroll compressors, and references [15 to 20] for rolling-piston-rotary compressors), such design guidelines for the maximum performance of reciprocating compressors, in contrast, are substantially less developed, even though the reciprocating compressor was among the earliest classical compression devices. Most dynamic analyses for the reciprocating compressor have focused on vibration characteristics, as listed in references [2l to 26]. The equation of motion of the rotating crankshaft and the inertia forces exciting vibration of the whole compressor were derived to calculate mechanical vibrations of a compact refrigerant compressor, synchronized with the crankshaft rotation [21-22]. Subsequently, higher frequency vibrations of the whole compressor, caused by elastic vibrations of the crankshaft, were experimentally identified and simulated in numerical studies [23-24]. Finally, higher frequency vibrations of the reed valves have been identified in experiments, and criteria for the onset of vibration and the volumetric similarity between reciprocating compressors and rolling-piston-rotary compressors have been developed [25-26].

Despite the relatively recent development and manufacturing of scroll compressors and rolling-piston-rotary compressors for use with refrigerants in cooling appliances in the early 1980s in Japan, optimal design guidelines for these compressors are more extensively developed. Indeed, the optimal design of these compressors was a major focus of the authors' research since their introduction. As a starting point, the equations of motion of compressor moving elements were derived to identify the constraint forces at each pair of compressor elements, ultimately permitting analysis in terms of the equation of motion of the rotating crankshaft. Further, the inertia forces exciting the vibration of the compressor body were derived and used to calculate the mechanical vibrations of the compressor, which are basically synchronized with the crankshaft rotation. Subsequently the mechanical, volumetric and overall compression efficiencies have been calculated, where the frictional losses, the compressed-gas leakage losses and the heat losses are all taken into consideration. As a result, optimal design guidelines for maximum efficiency have been established for scroll compressors [1-14] and for rolling-piston-rotary compressors [15- 20].

The present paper presents optimal design guideline for offset-type reciprocating compressors. Initially, the basic concept of optimal design to maximize the mechanical efficiency of off-set type reciprocating compressors is presented, wherein reference is made to those features reciprocating compressors have in common with scroll compressors and rotary compressors. For reciprocating compressors, there are many combinations of the piston stroke and the cylinder bore that result in the same suction volume. The frictional power loss at each pair of compressor elements depends not only upon the compression pressure and the inertia forces, but also upon the combinations of these major parameters. Consequently, the frictional power losses change, depending upon the selected combination of major parameters, thereby resulting in a different mechanical efficiency. Thus, selection of the optimum combination of major parameters is necessary to ensure maximum mechanical efficiency of the reciprocating compressor. Secondly, theoretical developments of the crankshaft rotation and the constraint forces at all pairs of compressor elements are briefly presented to derive the energy equation for reciprocating compressors. Thirdly, a sample calculation of the mechanical efficiency for a reciprocating refrigerant compressor with a suction volume of 6 cc and a induction motor is presented, along with the crankshaft speed fluctuation ratio. Calculations were made for a variety of combinations of major parameters, assuming friction coefficients, thus identifying the optimal combination to maximize the mechanical efficiency. Finally, a parametric study for a variety of non-dimensional off-set values is presented to demonstrate optimal off-set value.

2. Design Guideline to Maximize Mechanical Efficiency

For reciprocating compressors with the suction volume of V_s and cylinder bore *d,* the piston half-stroke *r* corresponding to the crank-arm rotating radius is given by the following expression:

$$r = \frac{2V_s}{\pi d^2} \tag{1}$$

Equation (1) is plotted in Figure 1(d) for values of V_s from 5 to 40 cc. The piston-crank mechanism is schematically shown in Figure 1(c), where the suction volume is shaded, for an assumed constant crank-arm to connecting-rod length ratio of 0.25. As the cylinder bore decreases toward the left side in Figure 1(c), the compressed gas force pushing the piston decreases, and hence the constraint forces against the gas force decrease at all pairs of compressor elements and, thus, the friction losses also decrease. On the other hand, with increasing piston stroke and decreasing cylinder bore, the inertia forces of the moving compressor elements increase resulting in greater constraint forces to oppose the inertia forces and, thus, increased friction losses. As a result, there is a critical combination of the piston

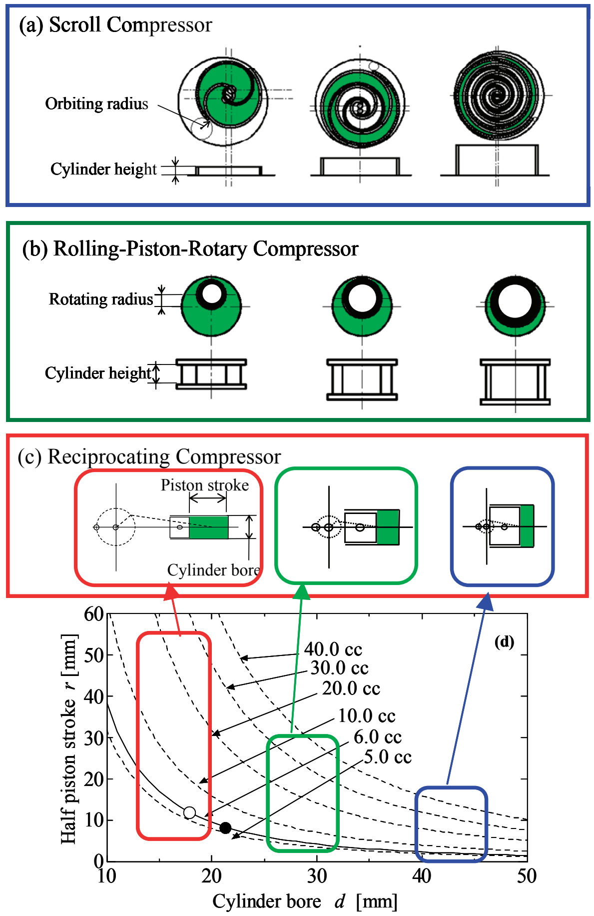

(d) Piston half-stroke vs. cylinder bore.

Figure 1 Combinations of piston stroke and cylinder bore for reciprocating compressors (c) with a suction volume from 5 cc to 40 cc(d), with a schematic comparison with major dimensions of scroll compressors (a) and rolling-piston-rotary compressors (b).

stroke and the cylinder bore, for which the friction loss will take on a minimum value, corresponding to a maximum mechanical efficiency.

The scroll compressor dimensions corresponding to the stroke and bore of the reciprocating compressor are the black-shaded orbiting radius of the scroll and the cylinder height, as shown in Figure 1(a). Similarly, for rolling-piston-rotary compressors, the corresponding dimensions are the black-shaded rotating radius of the rolling piston and the cylinder depth, as shown in Figure 1(b). As the green-shaded suction area increases with increasing orbiting radius for scroll compressors and with increasing rotating radius for rolling-piston compressors, the cylinder height must decrease to maintain a given suction volume. Similar to the above discussion of reciprocating compressors, it can be argued that both scroll and rolling-pin compressors have geometrical combinations of design dimensions for a given suction volume that produce minimum friction losses.

3. Theoretical Developments

A concentrated mass model of the offset piston-crank mechanism is presented in Figure 2(a), where the Cartesian coordinates (x-y-z) are introduced with the z-axis along the crankshaft center, the x-axis along direction of the reciprocating piston motion and the y-axis perpendicular to the x-z plane. The off-set value (in the y-direction) between piston center and x-axis is given by e. The crankshaft rotation, a significant parameter, is given by θ relative to the z-axis, and the connecting-rod rotation, an additional parameter, is given by ϕ. The piston displacement from the crankshaft center is represented by x_p. As shown in Figure 2(b), the crankshaft, loaded by the gas force P on the piston, is driven by motor torque M_D, and thereby the constraint forces and frictional torques appear, as represented by Q_x, Q_y and M_Q at the crankshaft, S_x, S_y and M_S at the crank pin, and T_x, T_y and M_T at the piston pin, in addition to the frictional force f on the piston side wall.

The equations of motion for each of the moving machine elements shown in Figure 2(b) can be derived: one for the piston reciprocating along x-axis, three for the connecting-rod moving in x and y directions and rotating with ϕ, and two for the crank arm moving in x and y directions, in addition to the main parameter, the crankshaft rotation θ. From the first 6 equations of motion, 6 constraint forces can be derived in terms of inertia forces in addition to the gas force, the frictional force on the piston side wall and the frictional moments at the crank pin and piston pin. Substituting the derived constraint forces into the last equation of motion for the rotating crankshaft, the equation of motion of the crankshaft rotation can be reduced to the following expression:

$$I_0'\ddot{\theta} + \left(-m_p'\ddot{x}_p\right)\left(x_p \tan\phi + e\right) + \alpha\frac{\cos\theta}{\cos\phi}I_c'\ddot{\phi} = M_D + P\left(x_p \tan\phi + e\right) - \left\{ f\left(x_p \tan\phi + e\right) + \frac{x_p}{\ell\cos\phi}M_S + \alpha\frac{\cos\theta}{\cos\phi}M_T + M_Q \right\} \quad (2)$$

The terms on the left-hand side represent the inertia torques, where the first term is for the rotating crankshaft with a modified moment of inertia I_0', the second is for the reciprocating piston with a modified mass m_p' and the third is for the rotating connecting-rod with a modified moment of inertia I_c'. On the right-hand side, the first term is the supplied motor torque M_D, and the second through sixth terms are the load torques: the second due to gas force P on the piston, the third due to frictional force f on the piston side wall and the fourth through sixth due to the frictional torques M_T, M_S and M_Q. The length ratio of the crank-arm to the connecting-rod is denoted by α.

The energy equation for the compressor can be derived by multiplying Equation (2) by a small angular displacement $d\theta$ and integrating each term over one revolution of the crankshaft. The energy supplied by the motor, E_s, goes primarily into the gas compression energy E_p and secondarily for the friction losses E_f at the cylinder wall, E_{MT} at the piston pin, E_{MS} at the crank pin and E_{MQ} at the crank journal:

$$E_s = E_p + E_f + E_{M_T} + E_{M_S} + E_{M_Q} \quad (3)$$

where

$$E_s = \int_{1-rev.} M_D(\dot{\theta})d\theta,\ E_p = \int_{1-rev.} P\left(x_p \tan\phi + e\right)d\theta,\ E_f = \int_{1-rev.} f\left(x_p \tan\phi + e\right)d\theta$$
$$E_{M_T} = \int_{1-rev.} \alpha\frac{\cos\theta}{\cos\phi}M_T d\theta,\ E_{M_S} = \int_{1-rev.} \frac{x_p}{l\cos\phi}M_S d\theta,\ E_{M_Q} = \int_{1-rev.} M_Q d\theta \quad (4)$$

Assuming Coulomb friction at each pair of elements, the friction forces can be derived by multiplying each resultant constraint force by each friction coefficient, thus resulting in

$$f = \delta_2\mu\left|T_y\right| \quad \text{, for TDC} < \theta < \text{BDC} : \delta_2 = +1,\ \text{BDC} < \theta < \text{TDC}: \delta_2 = -1)$$
$$M_T = \delta_3\mu_T\sqrt{T_x^2 + T_y^2}\cdot r_T \quad \left(-\frac{\pi}{2} \le \theta \le \frac{\pi}{2} \to \delta_3 = +1,\quad \frac{\pi}{2} \le \theta \le \frac{3\pi}{2} \to \delta_3 = -1\right)$$
$$M_S = \mu_S\sqrt{S_x^2 + S_y^2}\cdot r_S,\ M_Q = \mu_Q\sqrt{Q_x^2 + Q_y^2}\cdot r_Q \quad (5)$$

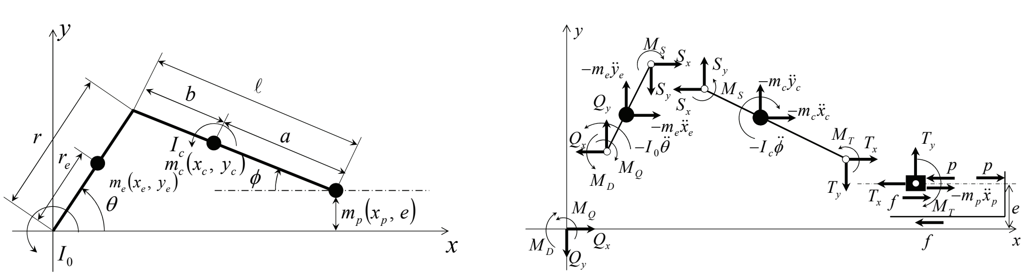

Figure 2 A representative model of off-set piston-crank mechanism: (a) concentrated mass system and introduction of major constants and variables; (b) constraint forces, frictional forces and frictional moments at all pairs of machine elements.

where the friction coefficients are represented by μ on the piston side wall, μ_T at the piston pin, μ_S at the crank pin and μ_Q at the crank journal. Consequently, the energy equation, Equation (3), can be utilized to express the mechanical efficiency η_m as follows:

$$\eta_m = \frac{E_s - \left(E_f + E_{M_T} + E_{M_S} + E_{M_Q}\right)}{E_s} \tag{6}$$

4. CALCULATED RESULTS

Calculations were undertaken for a compact reciprocating air-conditioning compressor, with a suction volume of 6 cc, driven by an induction motor. The major specifications are listed in Table 1. The piston half-stroke r_0 and the cylinder bore d_0 were 8.99 mm and 20.6 mm, respectively, and are plotted by the filled black circle in Figure 1(d). The rated conditions of operation were an average speed of 2950 rpm, with a suction pressure P_s of 0.0464 MPa and a discharge pressure P_d of 0.465 MPa. The gas compression in the cylinder is assumed to be polytropic with an index of n = 1.05. The values for friction coefficients, based on previous experience, were assumed to be in the raange μ = 0.1 ~ 0.5 and the remaining coefficients μ_T, μ_S and μ_Q take value of 0.02, 0.014 and 0.024. The non-dimensional off-set value ε is defined by

$$\varepsilon = \frac{e}{\ell} \tag{7}$$

which took on a value of -0.05.

Table 1 Major specifications of a compact reciprocating compressor for calculations.

Volume of Cylinder	V_s	6.0×10^3	[mm^3]
Average operation speed	f_{cycle}	2950	[rpm]
Bore of Cylinder	d_0	20.6	[mm]
Mass of Piston	m_{p0}	32.9×10^{-3}	[kg]
Mass of Connecting rod	m_{c0}	52.3×10^{-3}	[kg]
Length of Connecting rod	L_0	37.3	[mm]
Conn-rod gravity from small end	a_0	28.9	[mm]
Conn-rod gravity from big end	b_0	8.4	[mm]
Inertia moment of Conn-rod	I_{c0}	6.62×10^{-6}	[kgm^2]
Rotation radius of Crank pin	r_0	8.99	[mm]
Rotation radius of Crank gravity	r_{e0}	-2.24	[mm]
Inertia moment of Crankshaft	I_0	4.11×10^{-4}	[kgm^2]
Length ratio of Crank arm and Conn-rod	α	0.241	
Friction coeff. between piston and cylinder	μ	0.1~0.5	
Friction coeff. of crank journal	μ_Q	0.024	
Friction coeff. of crank pin	μ_S	0.014	
Friction coeff. of piston pin	μ_T	0.02	
Suction pressure	P_s	0.0464	[MPa]
Discharge pressure	P_d	0.465	[MPa]
Polytropic index	k	1.050	
Radius of Crank journal	r_Q	7.95	[mm]
Radius of Crank pin	r_S	7.00	[mm]
Radius of Piston pin	r_T	4.76	[mm]
non-dimensional off-set value	ε	-0.05	

The mechanical efficiency was calculated for a variety of combinations of the piston half-stroke r and the cylinder bore d for the fixed suction volume of 6.0 cc and for the specific crank-arm-to-connecting-rod length ratio α, fixed at 0.241. According to the selected combination, the piston mass m_p, the connecting-rod mass m_c and its moment of inertia I_c may be adjusted according to the following expressions:

$$m_p = \left(\frac{d}{d_0}\right)^2 m_{p0} \qquad m_c = \frac{l}{l_0} m_{co} \qquad I_c = \left(\frac{l}{l_0}\right)^2 I_{c0} \tag{8}$$

In contrast, the moment of inertia of the crankshaft, I_0, may not be adjusted, since the motor power does not change meaningfully, for the fixed suction volume.

4.1 Dynamic behavior

The equation of motion, Equation (2), for the rotating crankshaft can be numerically solved with an iterative calculation method. The 0th-order solution of crank angle θ is calculated from Equation (2) first, assuming zero frictional force and moments, and then the friction force and moments are calculated from Equation (5), and then substituted back into Equation (2) to obtain iteratively the higher-order solution of θ. Calculated results are shown in Figures 3(a) to 3(c), in which the acceleration, the velocity and the velocity fluctuation ratio over the crank angle θ for one revolution are presented. The third parameter is the cylinder bore d which varies from 10 mm to 50 mm. When d is larger, the acceleration exhibits a sharp negative peak at θ=-35^o, which exactly corresponds to the sharp peak in gas-compression torque curve, shown in Figure 3(d). Therefore, the gas compression is dominant over the acceleration. However, the acceleration curve becomes drastically different, when d becomes smaller. As d decreases, the negative peak becomes smaller and is lost in the large second-order noise which is clearly caused by the piston inertia torque shown in Figure 3(e), in addition to the connecting-rod inertia torque shown in Figure 3(f).

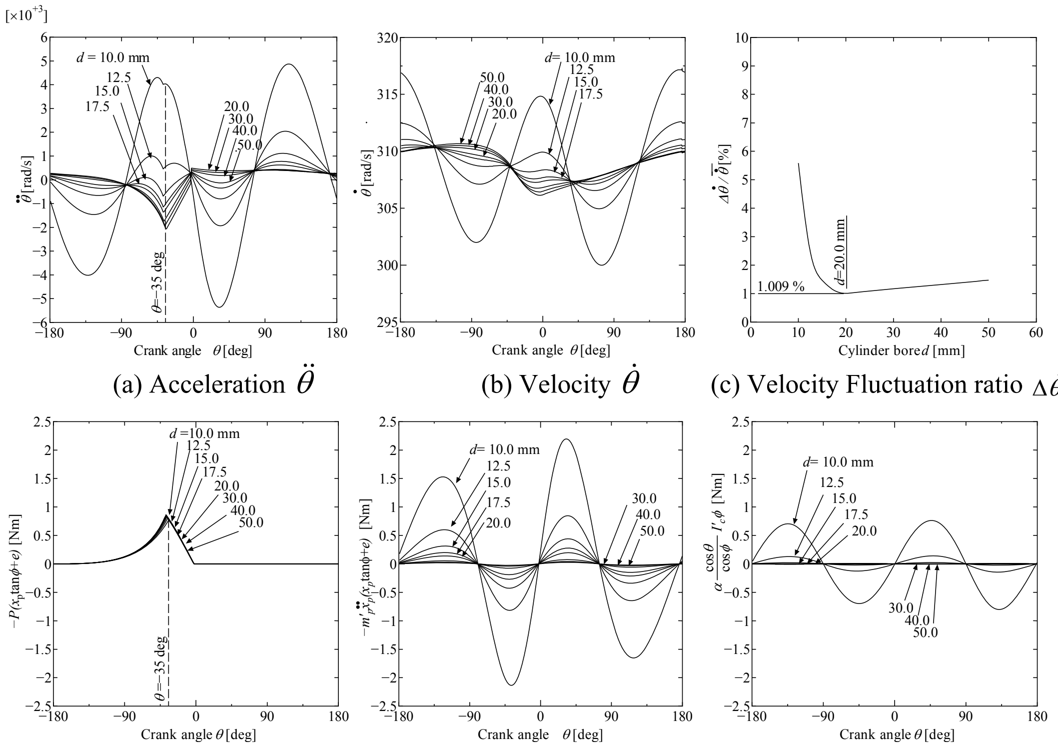

(a) Acceleration $\ddot{\theta}$ (b) Velocity $\dot{\theta}$ (c) Velocity Fluctuation ratio $\Delta\dot{\theta}/\bar{\dot{\theta}}$

(d) Gas compression (e) Piston inertia torque. (f) Connecting-rod inertia torque.

Figure 3 Resulting rotating behavior of the crankshaft, in addition to gas compression torque and inertia torques due to the piston and connecting-rod motions, for reciprocating compressors with V_S=6.0 cc.

As shown in Figure 3(e), the piston inertia torque reaches about -2.3 Nm at θ= -40°, a large enough value to offset substantially the gas-compression torque with its peak value of 1.0 Nm. The gas compression torque is naturally independent of *d*, as shown in Figure 3(d), while the inertia torques of the piston and the connecting-rod increases with decreasing *d* from 50 mm, as shown in Figures 3(e) and (f), further canceling the gas compression torque. Therefore, the velocity fluctuation decreases first, as shown in Figure 3(b), and correspondingly the velocity fluctuation ratio gradually decreases, as shown in Figure 3(c). However, when *d* becomes smaller than 20.0 mm, the inertia torques become dominant, thus resulting in a rapid increase in the velocity fluctuation ratio. The velocity fluctuation ratio exhibits its minimum value of 1.009% at *d* = 20.0 mm.

4.2 Mechanical Efficiency

The friction force *f* and the friction torques M_T, M_S and M_Q, given by functions of the crank angle θ, can be calculated from Equation (5), as shown by the solid line in Figure 4. The friction force *f* is determined with the side force on cylinder, T_y, and hence the curves for large cylinder bore *d* exhibit a sharp peak at θ=-35°, thus representing the dominance of the gas force effect. On the other hand the frictional torques M_T, M_S and M_Q exhibit a square form before the top dead center (θ= -2.3°), thus representing again the dominance of the gas force effect. As *d* decreases, the gas-force effect decreases and, in turn, the effect of inertia forces becomes dominant, as is clearly demonstrated in Figure 4(a) for *f*, in Figure 4(c) for M_S and in Figure 4(d) for M_Q. The inertia-force effect does not appear as large as was found for M_T shown in Figure 4(b). These significant results regarding inertia-force effects are consistent with Equation (7), which shows the inertia forces of the connecting-rod, the mass m_c and moment of inertia I_c become larger with decreasing *d*.

In Figure 4, the dashed line shows the friction force *f*, friction torque M_T, M_S and M_Q of the zero-off-set model. The friction force *f* for the off-set model is smaller, compared with that for the zero-off-set model. Especially, as the cylinder bore becomes larger, the negative maximum in the friction force is significantly reduced, due to a significant decrease in the side force against the cylinder wall, caused by the off-set. However, as shown in Figures 4(b), (c) and (d), the friction torques are not substantially affected at all by the off-set.

With these calculated results, the integrations in Equation (4) can be carried out to determine the friction power losses of off-set model shown by the solid line in Figure 5(a). Both the friction losses E_{MS} at the crank pin and E_{MQ} at the crank journal are relatively large, while E_{MT} at the piston pin is comparatively small. All three friction losses decrease with decreasing cylinder bore d, and first two exhibit their minima near d = 17.5 mm and then increase. In contrast, even if d decreases, E_f at the cylinder wall remains essentially constant and then starts to rapidly increase at d = 15 mm. As a result, the net loss E_F due to friction exhibits a minimum at d =17.5 mm, as shown in Figure 5(b), in which the motor power E_S and the gas-compression power E_P are also plotted. The dashed line in Figure 5(a) again represents the zero-off-set model. The friction losses E_{MQ}, E_{MS} and E_{MT} for the off-set model change very little relative to those for the zero-off-set model. However, the friction loss E_f for off-set model decreases slightly relative to that for the zero-off-set model.

Consequently, the mechanical efficiency η_m given by Equation (6) can be calculated and is plotted in Figure 5(c). As d decreases, η_m increases, exhibiting a maximum value of 87.01% at d = 17.5 mm, The filled black circle at d = 20.6

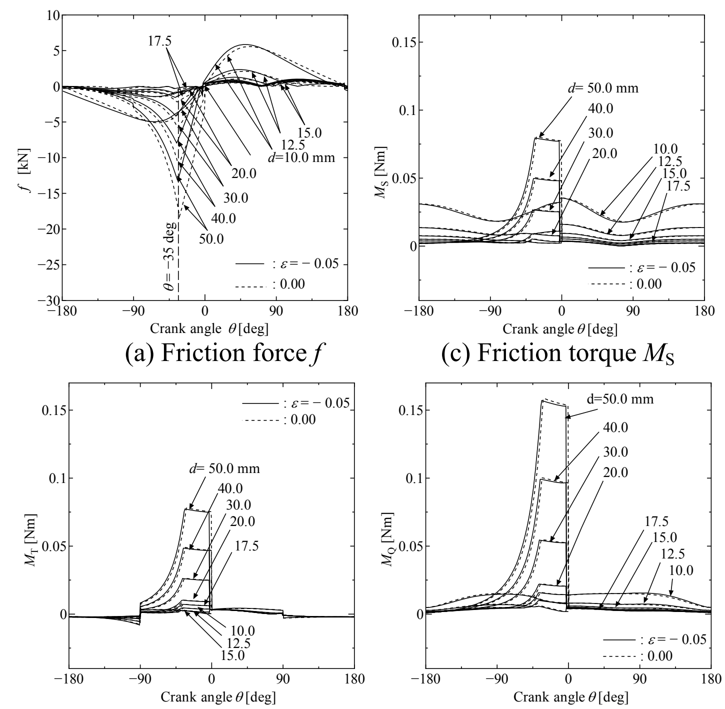

(a) Friction force f (c) Friction torque M_S

(b) Friction torque M_T (d) Friction torque M_Q

Figure 4 Friction force on the piston side wall and friction torques at the piston pin, the crank pin and the crankshaft.

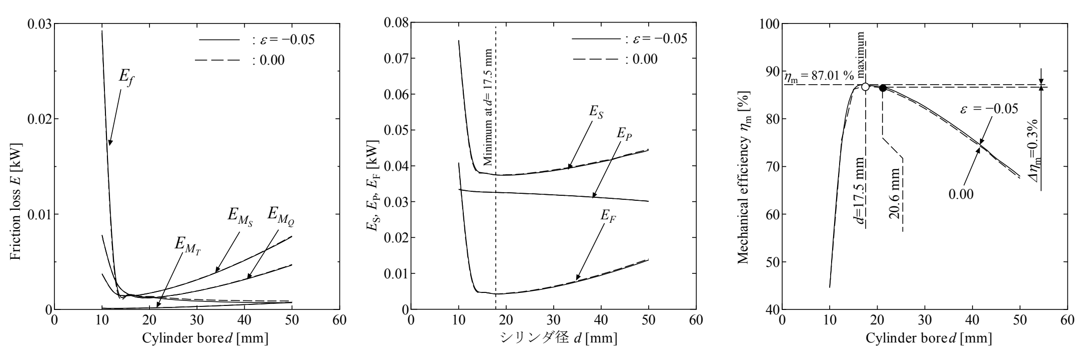

(a) Friction power losses (b) Motor power, gas compression power and net power loss due to frictions. (c) Mechanical efficiency

Figure 5 Calculated powers and resulting mechanical efficiency, for reciprocating compressors with V_s =6.0 cc.

mm represents the mechanical efficiency (86.71 %) of conventional compressor selected as the standard for present calculations, which is a significant 0.3 % lower than the maximum value. Schematic views of the piston-crank mechanism are shown for the conventional compressor with d =20.6 mm and for the optimal compressor with d = 17.5 mm in Figure 1(c), in order to make clear the difference in size. The length from crankshaft to cylinder head becomes larger for the optimal performance compressor, compared with that of the conventional compressor.
Furthermore, the mechanical efficiency for the zero-off-set model is 0.1% lower than that of the off-set model, due to a decrease in the friction loss at the piston side wall.

5. PARAMETRIC STUDY

In order to examine the effect of the non-dimensional off-set value ε that maximizes the mechanical efficiency, the value of ε was varied from -0.40 to 0.20. Calculated results for the maximum mechanical efficiency η_{max} as a function of non-dimensional offset ε are shown in Figure 6. When ε takes on a value of -0.05, the mechanical efficiency exhibits its highest value of 87.01% which is 0.1% higher than that for the zero-off-set model.

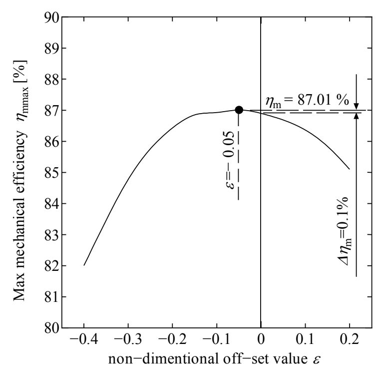

Figure 6 Variation of maximum mechanical efficiency with non-dimensional off-set

6. CONCLUSION

For a reciprocating refrigerant compressor with a suction volume of 6.0 cc, the optimal combination of the piston half-stroke r = 12.5 mm and the cylinder bore d =17.5 mm maximizes the mechanical efficiency reaching 87.01% with an optimal value of non-dimensional off-set of -0.05. Exceedingly large numbers of reciprocating compressors with small cooling capacity are being manufactured world-wide. The optimal design guidelines developed in this study should be carefully considered in the basic mechanism design to advance energy conservation and improve the global environment. Future studies are needed to examine the effects of selected design combinations on the leakage losses due to piston clearance and heat losses in the suction and compression processes.

NOMENCLATURE

a, a_0, b, b_0, l, l_0 Length of connecting-rod [mm]
d, d_0 Bore of cylinder [mm]
e Off-set value [mm]
E_S, E_P, E_f, E_{M_T}, E_{M_S}, E_{M_Q} Energy supplied by motor [W]
F Friction force between piston and cylinder [N]
I_0, I'_0 Moment of inertia of crankshaft and modified moment of inertia [kg m^2]
I_c, I_{c0}, I'_c Moment of inertia of connecting-rod and modified moment of inertia [kg m^2]
m_c, m_{c0} Mass of connecting-rod [kg]
m_p, m'_p, m_{p0} Mass mass of piston and modified mass [kg]
M_Q, M_S, M_T Frictional torques at crank journal, crank pin and piston pin [N m]
M_D Motor torque [N m]
P Gas force [N]
P_s, P_d Suction pressure and discharge pressure [MPa]
Q_x, Q_y, S_x, S_y, T_x, T_y Constraint forces at crank journal, crank pin and piston pin [N]
r, r_0 Rotating radius of crank pin [mm]

r_Q, r_S, r_T Radii of crank journal, crank pin and piston pin [mm]
V_s Suction volume of cylinder [mm^3]
x_p Piston displacement [m]
α Specific length ratio of crank arm to connecting-rod [-]
θ, ϕ Rotating angle of crankshaft and connecting-rod [rad]
μ, μ_Q, μ_S, μ_T Friction coefficients at cylinder wall, crank journal, crank pin and piston pin [-]
ε Non-dimensional off-set value [-]

REFERENCES

1. Ishii, N., Fukushima, M., Sawai K., Sano, K., Imaichi, K., 1988, Dynamic Behavior of a Scroll Compressor (Dynamic Analysis), JSME Int. Journal, Ser 3, pp. 58-67.
2. Ishii, N., Yamamura, M., Morokoshi, H., Fukushima, M., Yamamoto, S., Sakai, M., 1988, On the Superior Dynamic Behavior of a Variable Rotating Speed Scroll Compressor, *Proc. of Int. Comp. Engrg. Conf. at Purdue*, pp. 75-82.
3. Ishii, N., Yamamura, M., Morokoshi, H., Muramatsu, S., Sawai, K., Osaka, M., Yamamura, M., 1987, Mechanical Efficiency of Various Large Capacity Scroll Compressors, *Proc. of 17th Int. Congress of Refrigeration*, Wien Austria, pp. 468-474.
4. Ishii, N., Yamamura, M., Muramatsu, S., Yamamoto, S., Sakai, M., 1990, Mechanical Efficiency of a Variable Speed Scroll Compressor, *Proc. of Int. Comp. Engrg. Conf. at Purdue*, Vol.1, pp. 192-199.
5. Ishii, N., Yamamoto, S., Muramatsu, S., Yamamura, M., Takahashi, M., 1992, Optimum Combination of Parameters for High Mechanical Efficiency of a Scroll Compressor, *Proc. of Int. Comp. Engrg. Conf. at Purdue*, pp. 118a1-118a8.
6. Ishii, N., Yamamura, M., Muramatsu, S., Yamada, S., Takahashi, M., 1994, A Study on High Mechanical Efficiency of a Scroll Compressor with Fixed Cylinder Diameter, *Proc. of Int. Comp. Engrg. Conf. at Purdue*, Vol.2, pp. 677-682.
7. Ishii, N., Sakai, M., Sano, K., Yamamoto, S., Otokura, T., 1996, A Fundamental Optimum Design for High Mechanical and Volumetric Efficiency of Compact Scroll Compressors, *Proc. of Int. Comp. Engrg. Conf. at Purdue*, Vol. II, pp. 639-644.
8. Ishii, N., Yamamoto, S., Sano, K., Sawai, K., Hiwata, A., Nakamoto, T., Kawano, H., 2002, Efficiency Simulations of a Compact CO_2 Scroll Compressor and Its Comparison with Same Cooling Capacity R410A Scroll Compressor, *Proc. of Int. Comp. Engrg. Conf. at Purdue*, C22-2(CD-ROM).
9. Ishii, N., Kawamura, S., Yamamoto, S., Sawai, K., Hiwata, A., Nakamoto, T., Kawano, H., Ting, K S., 2002, Efficiency Simulations with Consideration of Heat Losses of R410 Compact Scroll Compressor for Its Optimal Performance, *Proc. of Int. Comp. Engrg. Conf. at Purdue*, C22-3(CD-ROM).
10. Oku, T., Ishii, N., Anami, K., Knisely, C.W., Sawai, K., Morimoto, T., Hiwata, A., 2008, Theoretical Model of Lubrication Mechanism in the Thrust Slide-Bearing of Scroll Compressors, HVAC&R Research Journal ASHRAE Vol.14, No.2, pp. 239-258.
11. Ishii, N., Oku, T., Anami, K., Knisely, C.W., Sawai, K., Morimoto, T., Iida, N., 2008, Experimental Study of the Lubrication Mechanism for Thrust Slide Bearings in Scroll Compressors, HVAC&R Research Journal ASHRAE Vol.14, No.3, pp. 453-465.
12. Ishii, N., Oku, T., Anami, K., Knisely, C.W., Sawai, K., Morimoto, T., Iida, N., 2008, Optimal Performance Design Guidelines of Thrust Slide-Bearing in Scroll Compressors for Maximum Efficiency, *Proc. of Int. Comp. Engrg. Conf. at Purdue*, 1428, pp. 1-8.
13. Ishii, N., Oku, T., Anami, K., Knisely, C.W., Sawai, K., Morimoto, T., Fujiuchi, K., 2008, Effects of Surface Roughness upon Gas Leakage Flow Through Small Clearances in CO_2 Scroll Compressors, *Proc. of Int. Comp. Engrg. Conf. at Purdue*, 1429, pp. 1-8.
14. Ishii, N., Oku, T., Anami, K., Knisely, C.W., Sawai, K., Morimoto, T., Iida, N., 2008, Optimal Performance Development of High-Pressure Type Ammonia Scroll Compressors for Maximum Efficiency, *Proc. of Int. Comp. Engrg. Conf. at Purdue*, 1425, pp. 1-8.
15. Imaichi, K., Fukushima, M., Muramatsu, S., Ishii, N., 1982, Vibration Analysis of Rotary Compressors, *Proc of Int. Comp. Engrg. Conf. at Purdue*, pp. 275-282.
16. Ishii, N., Imaichi, K., Muramatsu, S., Fukushima, M., Matsunaga, H., 1984, The Study of Rolling Piston, Rotary Compressor Dynamic Behavior with Stopping to Reduce Noise and Vibration Level, *Proc. of Int. Comp. Engrg. Conf. at Purdue*, pp. 1-8.

17. Ishii, N., Fukushima, M., Yamamura, M., Muramatsu, S., Sano, K., Sakai, M., 1989, The High Mechanical Efficiency of Rolling–Piston Rotary Compressors, *Proc of the 2nd World Congress on Heating Ventilating*, Refrigeration and Air Conditioning(CLIMA2000), Sarajevo, Yugoslavia, pp. 91-96.
18. Ishii, N., Fukushima, M., Yamamura, M., Fujiwara, S., Kakita, S., 1990, Optimum Combination of Dimensions for High Mechanical Efficiency of a Rolling–Piston Rotary Compressor, *Proc of Int. Comp. Engrg. Conf. at Purdue*, Vol. 1, pp. 418-424.
19. Ishii, N., Morita, N., Ono, M., Yamamoto, S., Sano, K., 2000, Net Efficiency Simulations of Compact Rotary Compressors for Its Optimal Performance, *Proc. of Int. Comp. Engrg. Conf. at Purdue*, Vol. I, pp. 475-482.
20. Ishii, N., Morita N., Kurimoto, M., Yamamoto, S., Sano K., 2000, Calculations for Compression Efficiency Caused by Heat Transfer in Compact Rotary Compressors, *Proc. of Int. Comp. Engrg. Conf. at Purdue*, Vol. I, pp. 467-474.
21. Ishii, N., Imaichi, K., Kagoroku, N., Imasu, K., 1975, Vibrations of a Small Reciprocating Compressor, Design Engng. Technical Conf., Washington D. C, ASME, pp. 1-12.
22. Imaichi, K., Ishii, N., Imasu, K., Murai, M., 1979, A Device for Stopping Single-Cylinder Reciprocating Compressors Silently by Greatly Reducing Vibrations, *Proc. of 15th Int. Congress of Refrigeration*, Vol. II, pp. 727-733.
23. Ishii, N., Imaichi, K., Muramatsu, S., Fukushima, M., 1983, A Computer Simulation of Higher Frequency Vibrations of A Reciprocating Compressors, *Proc. of 16th Int. Congress of Refrigeration*, pp. 418-423.
24. Imaichi, K., Ishii, N., Imasu, K., Muramatsu, S., Fukushima, M., 1984, A Vibration Source in Refrigerant Compressors, Transactions of the ASME, Journal of Vibration, Stress, Reliability and Design, Vol. 106, pp. 122-128.
25. Ishii, N., Fukuoka, H., Matsunaga, H., Fukushima, M., Nakazumi, K., 1993 Dynamic Stability Criterion for Reed Valves in Refrigerant Compressors, JSME Int. Journal, Ser C, Vol. 36, No.1, pp. 69-76.
26. Ishii, N., Hitotsubashi, M., Yamamoto, S., Matsunaga, H., Hashimoto, T., Sano K., 1998, Volumetric Similarity for Vibrations of Reed Valve in Refrigerant Compressors, *Proc. of Int. Comp. and Their Systems*, London, pp. 99-104,

7. ACKNOWLEDGEMENTS

The authors would like to express their sincere gratitude to Mr. ***Haruyuki Ishiou***, Vice President, and Mr. ***Masahiro Atarashi***, Director of Appliance Development Center, Corporate Engineering Division, and Mr. ***Shuichi Yamamoto***, Director, Air Conditioning Devices Business Unit, Home Appliances Corporation, Panasonic Co., Ltd., for their collaborative support in carrying out this work and their permission to publish this study.